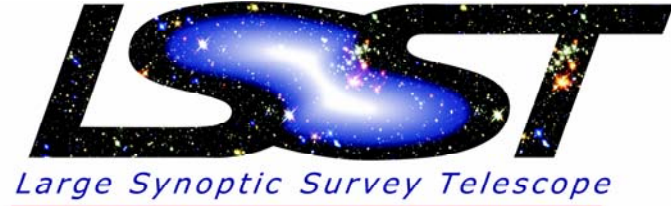


# Supernovae and Cosmic Shear as Complementary Probes of Dark Energy

A. Albrecht, L. Knox (UC Davis), Y.-S. Song (U Chicago), J.A. Tyson, D. Wittman, and H. Zhan (UC Davis)



Weak lensing observations and supernova observations, combined with CMB observations, can both provide powerful constraints on dark energy properties. We find luminosity distances inferred from 2000 supernovae and large-scale ( $l < 1000$ ) angular power spectra inferred from redshift-binned cosmic shear maps of half of the sky place complementary constraints on  $w_0$  and  $w_a$  where the dark energy equation of state  $w(z) = w_0 + w_a(1 - a)$ . Further, each set of observations can constrain higher-dimensional parameterizations of  $w(z)$  and constrains these in different ways. To quantify these abilities we consider eigenmodes of the  $w(z)$  error covariance matrix. The best-determined mode for each dataset has a standard deviation of about 0.03. This error rises quite slowly with increasing eigenmode number for the lensing data, reaching one only by the 7th mode. The eigenmode shapes have interesting differences indicating that lensing is better at probing higher  $z$  while supernovae have their chief advantage at lower  $z$ . If the prior of a flat geometry is relaxed, the weak lensing derived constraints on dark energy are expected to be less affected than the supernova constraints.

## 1. Introduction

• **Complementary Probes** Given the importance of the dark energy mystery and the challenges to constraining its properties, the diversity of methods to probe it is a blessing. Here we focus on two methods: weak lensing (WL) shear power spectra and supernova (SN) luminosity distances. Each of these highly different types of observations are potentially powerful probes of dark energy. In particular we examine the complementary nature of their statistical errors. See posters 26.5–26.7 and 26.35 for other complementary methods of baryon acoustic oscillations, SNe, and WL.

## 2. Models of the Data

• **Cosmic Shear** For the 20,000 deg<sup>2</sup> LSST WL survey, we assume a galaxy redshift distribution for a limiting magnitude in  $r$ -band of 26.5 (AB mag) inferred from observations with the Subaru telescope (Nagashima et al. 2002). The shape of this distribution is well-described by the following analytic form:

$$\begin{aligned} dn/dz &= z^{1.3} \exp[-(z/1.2)^{1.2}] \text{ for } z < 1 \\ dn/dz &= z^{1.1} \exp[-(z/1.2)^{1.2}] \text{ for } z > 1. \end{aligned}$$

We use this distribution with the modification that half of the galaxies in the  $1.2 < z < 2.5$  range are discarded as undetectable. The amplitude of the distribution is such that, after this cut, the number density of galaxies is 65 per square arcmin.

We further assume that the galaxies can be divided, by photometric redshift estimation, into eight different redshift bins: [0-0.4], ..., [2.8-3.2] and that for multipoles  $40 < l < 1000$  systematic errors are small. While this last assumption is consistent with recent data from new technology telescopes, all-sky simulations will be necessary. Finally, we assume that the shape noise (expressed as a per-component rms shear) is given by  $\gamma_{\text{rms}}(z) = 0.15 + 0.035 z$ .

For more details of the data modeling, see Song & Knox (2004).

• **Supernovae.** For the SN survey we assume 2000 SNe distributed in redshift as described in Kim et al. (2004) as a baseline *SNAP* SN survey. In addition, we assume measurement of 100 local SNe. To our cosmological parameter set, detailed below, we add a SN luminosity calibration parameter. Systematic errors are not included explicitly, but the *SNAP* baseline survey is designed not to reduce statistical errors far below the expected systematic error limits.

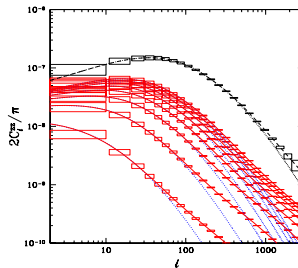


**Figure 1: Shear Power Spectra**  
The shear-shear auto power spectra. The 8 solid curves are the shear power spectra from each of the eight galaxy source planes. Dotted curves are the linear theory approximation. The source plane redshift intervals are all of width 0.4 and are centered on, from bottom up: 0.2, 0.6, 1.0, 1.4, 1.8, 2.2, 2.6, and 3.0. The error boxes are forecasts for LSST. The top dashed curve is the shear power spectrum for the CMB source plane. Its error boxes are forecasts for CMBpol.

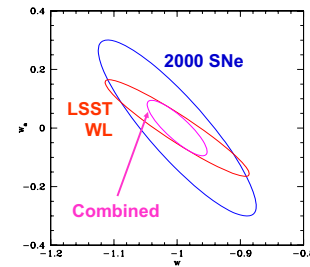


**Figure 2: Error Forecasts for  $w_0$  and  $w_a$**  One sigma error contours in the  $w_0$ - $w_a$  plane for LSST, 2000 SNe, and the combination (as labeled), where  $w(z) = w_0 + w_a(1 - a)$ . A joint analysis with three-point shear correlations, baryon oscillations, and cluster counting can yield higher precision. Note, however, that uncertainties of the photometric redshift error distribution will degrade the constraints (e.g. Ma, Hu, & Huterer 2005).

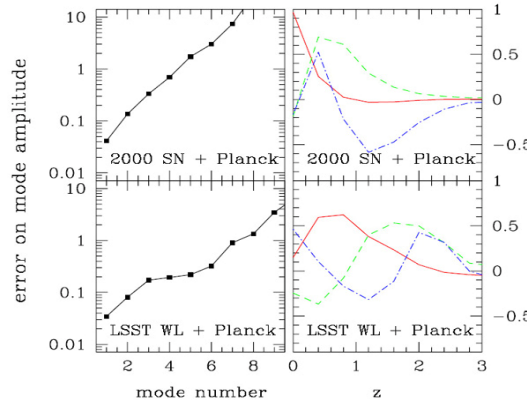


**Figure 3: Principle Components of  $w(z)$**  Eigenvalues (left column) and first three eigenmodes (right column) of the  $w(z)$  error covariance matrix for LSST + Planck and 2000 SNe + Planck. The large contributions to the eigenmodes from the highest redshift-bin are an artifact of that bin being much broader than the rest, extending all the way to the last-scattering surface.

## 3. Models of Cosmology

• **The Parameter Set.** We take our [non- $w(z)$ ] set to be  $P = \{\omega_m, \omega_b, \omega_\Lambda, \theta_s, z_{\text{re}}, k^3 P_\zeta(k), n_s, n_s', y_{\text{He}}\}$ , with the assumption of a flat universe. The first three of these are the densities today (in units of  $1.88 \times 10^{-29} \text{g cm}^{-3}$ ) of cold dark matter plus baryons, baryons, and massive neutrinos. We assume two massless species and one massive species. The next is the angular size subtended by the sound horizon on the last-scattering surface. The Thompson scattering optical depth for CMB photons,  $\tau$ , is parameterized by the redshift of reionization  $z_{\text{re}}$ . The primordial potential power spectrum is assumed to be a near power-law with spectral index  $n_s(k) = n_s(k_1) + n_s' \ln(k/k_1)$  and  $k_1 = 0.05 \text{ Mpc}^{-1}$ . The fraction of baryonic mass in Helium (which affects the number density of electrons) is  $y_{\text{He}}$ . We Taylor expand about  $P = \{0.146, 0.021, 0, 0.6, 6.3, 6.4 \times 10^{11}, 1, 0, 0.24\}$ . The Hubble constant for this model is  $H_0 = 65.5 \text{ km s}^{-1} \text{ Mpc}^{-1}$ .

•  **$w(z)$  in redshift bins.** To deepen our understanding of how these surveys are constraining dark energy, we have examined how they constrain the function  $w(z)$ , rather than its simple parameterization by  $w_0$  and  $w_a$ . We proceed by binning  $w(z)$  in redshift bins and then identifying the eigenmodes and eigenvalues of the binned  $w(z)$  error covariance matrix as was done for SNe by Huterer & Starkman (2003).

## 4. Results

We particularly emphasize the eigenmode/eigenvalue results. We see a striking difference in the modes for 2000 SNe vs. the modes for LSST WL: those for LSST stretch out to higher  $z$ . The reason for this is that lensing is less sensitive to the growth factor at the lower redshifts where the source density in a given redshift bin is small and the lensing window (for sources at higher  $z$ ) is also small. Thus the SNe are better at detecting changes in  $w(z)$  at lower  $z$  and LSST tends to be better at detecting changes at higher redshift.

LSST and 2000 SNe also have strikingly different eigenvalue spectra. The error on the amplitude of the best determined mode is quite similar for each ( $\sim 0.03$ ). But the 2000 SNe spectrum is much steeper. LSST has six modes with  $\sigma < 0.5$ , whereas 2000 SNe has three.

It has been shown for SNe ( $z < 2$ ) that the constraints on  $w_0$  and  $w_a$  can loosen considerably if one relaxes the flatness assumption (Weller & Albrecht 2001; Linder 2005). We do not expect the same level of degradation to LSST WL results, because high- $z$  data will enable LSST WL to place strong constraints on curvature (see poster 26.5 for results with baryon acoustic oscillations).

The LSST research and development effort is funded in part by the National Science Foundation under Scientific Program Order No. 9 (AST-0551161) through Cooperative Agreement AST-0132798. Additional funding comes from private donations, in-kind support at Department of Energy laboratories and other LSSTC Institutional Members.

National Optical Astronomy Observatory  
Research Corporation  
The University of Arizona  
University of Washington

Brookhaven National Laboratory  
Harvard-Smithsonian Center for Astrophysics  
Johns Hopkins University  
Las Cumbres Observatory, Inc.

Lawrence Livermore National Laboratory  
Stanford Linear Accelerator Center  
Stanford University  
The Pennsylvania State University

University of California, Davis  
University of Illinois at Urbana-Champaign